
Proceedings of Ninth World Conference on Earthquake Engineering
August 2-9, 1988, Tokyo-Kyoto, JAPAN (Vol.II)

3-1-6

SPATIAL INTERPOLATION OF ARRAY GROUND MOTIONS FOR ENGINEERING ANALYSIS

N. Abrahamson
Bechtel Civil Inc., San Francisco, CA, USA

SUMMARY

The dimensions of most strong motion arrays are larger than the dimensions of most structures so that the recorded motions can not be used directly to model the spatial variation of ground motion over the dimensions of interest to engineers. This paper presents a method for the spatial interpolation of strong motion array recordings to produce closely spaced time histories that can be used directly in engineering analyses.

INTRODUCTION

It has long been known that strong motion recordings from buildings show some filtering of the high-frequency energy compared to free-field recordings (e.g. Housner, 1957 (ref. 1)). Only part of the filtering can be explained by soil-structure interaction. The remaining filtering may be due to the spatial variation of the ground motion over the base of the structure. For example, Newmark et al., 1978 (ref. 2) analyzed the response of the Hollywood storage building to the 1971 San Fernando Earthquake. They showed that by averaging the free-field accelerogram over a time window of length τ, they could reasonably reproduce the high-frequency reduction observed in the foundation's response. The idea behind Newmark's analysis is that the high frequency ground motion varies over the dimension of the foundation and, as a result, the foundation acts as a low pass filter. Since this important study, there has been interest in estimating the spatial variation of ground motion over distances comparable to large structures and in determining its effect on structure response.

Ideally, dense array recordings can be used to directly measure the spatial variation of strong ground motion and its effects on foundation response; however, as noted by Luco and Wong, 1986 (ref. 3), there are two major limitations in most of the available strong motion array recordings: some strong motion arrays are linear while foundations are two dimensional and separations between instruments in strong motion arrays are typically larger than the dimensions of most foundations. These fundamental limitations of the available strong motion array recordings have led some authors to use analytic correlation functions to describe the spatial variation of the ground motion rather than using actual array recordings (e.g. ref. 3).

Despite the relatively large dimensions of most strong motion arrays, array recordings still provide valuable information on the seismic wavefield. This paper describes a simple method that uses array analysis techniques to parameterize the array recordings and then reconstruct the wavefield at closely spaced grid points. These interpolated ground motions can be used for engineering analysis of large structures.

METHOD

It is assumed that the recorded wavefield can be described by deterministic plane wave propagation from multiple sources (signals) and random effects (noise). Conventional frequency-wavenumber (f-k) analysis is used to decompose the recorded wavefield into its constituent signals and noise. A description of the f-k algorithm used in this study is given in reference 4. After the f-k analysis, the recorded ground motion, $u(x_m,\omega)$, can be written as

$$u(\vec{x}_m, \omega) = \sum_{j=1}^{q} A_j(\omega) \exp(i\vec{k}_j \cdot \vec{x}_m + \theta_j) + \varepsilon(\vec{x}_m,\omega) , \qquad (1)$$

where ω is frequency, $\vec{x}_m$ is the location of the m^{th} station, q is the number of plane wave signals, $A_j(\omega)$, $\vec{k}_j$, and θ_j are the amplitude, wavenumber and phase of the j^{th} signal, and $\varepsilon(\vec{x}_m,\omega)$ is the noise at the m^{th} station.

The interpolated ground motions are estimated by recombining the signals and the noise. The ground motion at position $\vec{x}$ is estimated by

$$u(\vec{x}, \omega) = \sum_{j=1}^{q} A_j(\omega) \exp(i\vec{k}_j \cdot \vec{x} + \theta_j) + \overline{B}_\varepsilon(\vec{x},\omega) \exp[i\phi_\varepsilon(\vec{x},\omega)] , \qquad (2)$$

where $\overline{B}_\varepsilon$ and ϕ_ε are estimates of of the Fourier amplitude and phase of the noise. The amplitude term, $\overline{B}_\varepsilon$, is the weighted mean amplitude of the noise given by

$$\overline{B}_\varepsilon(\vec{x},\omega) = \frac{\sum_{m=1}^{N} w(\vec{x}-\vec{x}_m,\omega)\, B_\varepsilon(\vec{x}_m,\omega)}{\sum_{m=1}^{N} w(\vec{x}-\vec{x}_m,\omega)} , \qquad (3)$$

where w is the weight function described below. The phase term, ϕ_ε, is a random sample from a normal distribution with the mean given by the phase of

$$\overline{\varepsilon}(\vec{x},\omega) = \frac{\sum_{m=1}^{N} w(\vec{x}-\vec{x}_m,\omega)\, \varepsilon(\vec{x}_m,\omega)}{\sum_{m=1}^{N} w(\vec{x}-\vec{x}_m,\omega)} , \qquad (4)$$

and the variance is computed from the noise phases.

The weights, w, are chosen to be a function of the coherency of the noise:

$$w(\vec{x}-\vec{x}_m,\omega) = \tanh^{-1}\left|\mathrm{Re}[\gamma_\varepsilon(\vec{x}-\vec{x}_m,\omega)]\right| , \qquad (5)$$

where γ_ε is the complex noise coherence and Re denotes the real part. Using only the real part of the complex noise coherency results in an "unlagged" coherency. The $\tanh^{-1}$ transformation comes from statistical studies of coherency (ref. 5). It is used here for the weights because it gives more weight to nearby stations than a simple $|\gamma|$ weight. In particular, $\tanh^{-1}|\gamma| \to \infty$ as $|\gamma| \to 1$ so that an interpolated time history will approach the recorded time history as the interpolation location approaches a recording station location.

The coherency, γ_ε, is computed for the noise terms and an empirical relation is derived to describe its dependence on station separation distance and wave frequency. Note that the method is earthquake specific: individual empirical relations are derived for each earthquake studied.

EXAMPLE

An example of the method is presented using recordings from the SMART 1 strong motion array in Taiwan. The SMART 1 array and the earthquake recordings used in this example are described below.

SMART 1 Array: The SMART 1 array is located in northeastern Taiwan. The configuration of the 37 force-balance triaxial accelerometers in the main array is shown in Figure 1. A complete description of the array is given in reference 6. The main array consists of a center station and three concentric rings of radii 200m, 1000m, and 2000m with twelve approximately equally spaced stations on each ring. In this paper, only the inner ring stations and the central station are used in the spatial interpolation.

Selected Data: The SMART 1 recordings from the magnitude 5.8 January 16, 1986 earthquake are used. The epicentral distance for this event is 22 km. The accelerograms from the inner ring are shown in Figure 2. For this example, only the 5 second S wave window on the NS component is used. For a complete analysis, the P wave and surface waves would also be considered.

F-K Analysis: The f-k spectrum is computed for frequencies from 0.4 to 10 Hz in 0.6 Hz steps. Spectra at frequencies above 10 Hz were not used because they are dominated by noise. A sample wavenumber spectrum is shown in Figure 3. This wavenumber spectrum is for a frequency of 4.0 Hz. Note that there are three main peaks in the spectrum. The locations of these peaks indicate the wavenumbers of the signals.

Noise Coherency: After determining the signal wavenumbers and amplitudes, the noise terms, $\varepsilon(\omega,x_m)$ are estimated for each station. These noise terms are then used to estimate the noise coherency, γ_ε. The noise coherencies computed for this example are shown in Figures 4a-b. For ease of presentation, the coherencies shown in Figures 4a-b have been smoothed over four station separation bins: 50-150 m, 150-250 m, 250-350 m, and 350-450 m. Note that the noise coherency does not appear to be frequency dependent. This lack of frequency dependence is observed because the signals have been removed. In contrast, the coherency for total accelerogram (signals and noise) are strongly dependent on frequency (ref. 7).

Various functional forms of the regression equation have been used in earlier studies of seismic wave coherency (refs. 8, 9, 10). However, these studies are for signal plus noise coherency and do not use the $\tanh^{-1}$ transformation. The goal of this study is to predict ground motions at short station spacings. This requires that the coherency (weighting) is appropriate for short station spacings. By definition, at zero station spacing, $\tanh^{-1}|\mathrm{Re}[\gamma]| \rightarrow \infty$. I have approximated this constraint by using a value of 4.0 rather than ∞. With this constraint in mind, examination of the distance dependence of the noise coherency shown in Figure 4a suggests the following functional form

$$\tanh^{-1}\left|\mathrm{Re}[\gamma_\varepsilon(\xi)]\right| = (4-c_1)\, e^{b\xi} + c_1 + c_2\xi, \qquad (6)$$

where $\xi = |\vec{x}-\vec{x}_m|$. It should be noted that this function does not work well for extrapolations to large station spacings. The estimated parameters from a non-linear regression analysis are as follows: c1=0.44, c2=0.01, b=-29.4. The standard error of a single observation is 0.34. The noise coherency model is plotted in Figure 5.

Interpolated Motion: The interpolated motions are estimated using Eq. (2) with weights given by the coherency function shown in Figure 5.. Seven interpolated motions between stations C-00 and I-12 are shown in Figure 5. These two stations are 200 meters apart. Note how the interpolated

motions become similar to the recorded motion as the interpolation point approaches a recording station location.

CONCLUSIONS

The proposed method allows estimation of closely spaced input ground motions from strong motion array recordings. The method models both deterministic wave propagation and random effects; additionally, it can accommodate multiple seismic sources and multiple wave types.

REFERENCES

1. Housner, G. W., "Interaction of building and ground during and earthquake", Bull. Seism. Soc. Am., **47**, 179-186, (1957).
2. Newmark, N. M., Hall, W. J., and Morgan, J. K., "Building response and free field motion in earthquakes", Proc. Sixth World Conf. Earth. Engin., New Delhi, India, 972-978, (1978).
3. Luco, J. E. and Wong, H. L., "Response of a rigid foundation to a spatially random ground motion", Earth. Engin. Struct. Dyn., **14**, 891-908, (1986).
4. Abrahamson, N. A. and Bolt, B. A., "Array analysis and synthesis mapping of strong seismic motion", in Strong Motion Synthetics, B. Bolt ed., 55-73, (1987).
5. Brillinger, D. R., Time Series, data analysis and theory, Expanded edition, Holden-Day, San Francisco, (1981).
6. Bolt, B. A., Loh, C. H., Penzien, J., Tsai, Y. B., and Yeh, Y. T, "Preliminary report on the SMART 1 strong motion array in Taiwan", Univ. Calif., EERC Report No. UCB/EERC82/13, (1982).
7. Abrahamson, N. A., "Empirical models of spatial coherency of strong ground motion", Proc. Second Workshop on Strong Motion Arrays, Taipei, Taiwan, (1988). In press.
8. Harada, T., "Probabilistic modeling of spatial variations of strong earthquake ground displacements", Eighth World Conf. Earth. Engin., San Francisco, **II**, 605-612, (1984).
9. Smith, S. W., Ehrenberg, J. E. and Hernandez, E. N., "Analysis of the El Centro differential array for the 1979 Imperial Valley earthquake", Bull. Seism. Soc. Am., **72**, 237-258, (1982).
10. Harichandran, R. S., "Local spatial variation of ground motion", ASCE Proc. Earthquake Engineering and Soil Dynamics II - Recent Advances in Ground-Motion Evaluation, 203-217, (1988).

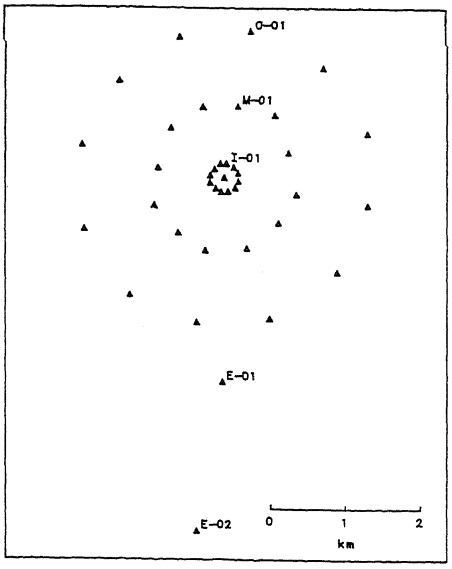

Figure 1. Configuration of the SMART 1 array.

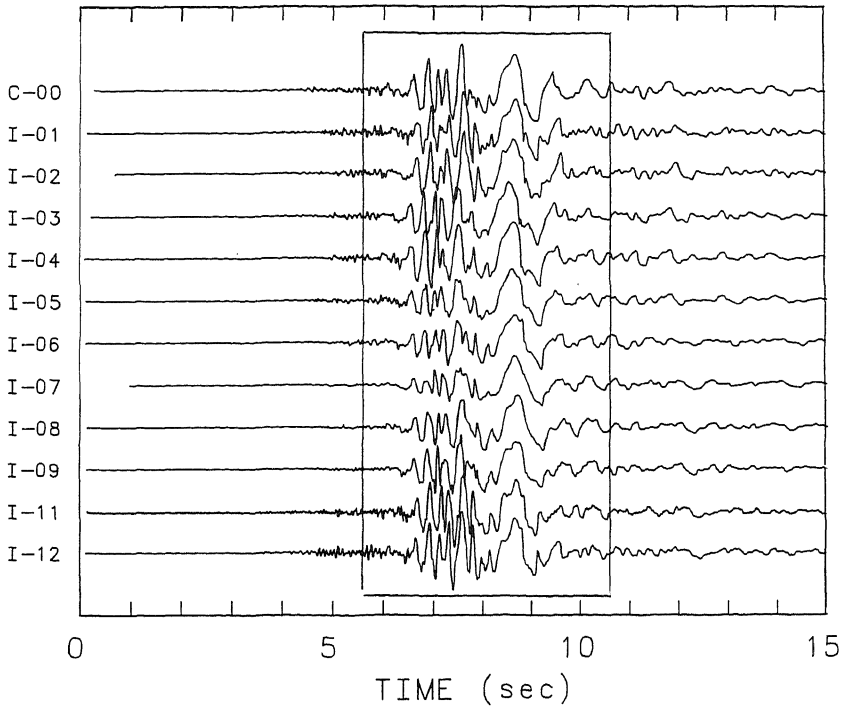

Figure 2. Array recordings used in the analysis.
The selected 5 second window is shown by the box.

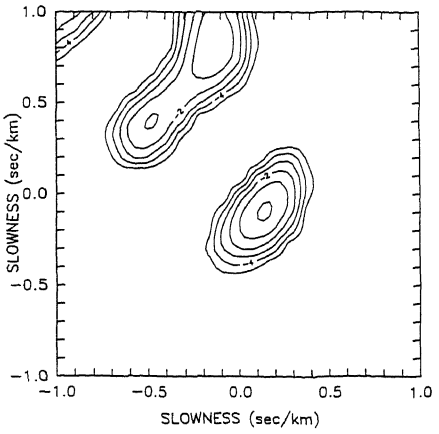

Figure 3. Sample wavenumber spectrum (4 Hz).

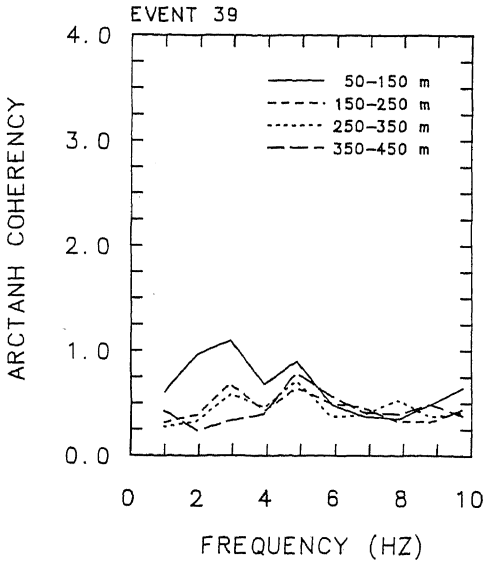

Figure 4a. The smoothed noise coherency plotted as a function of frequency.

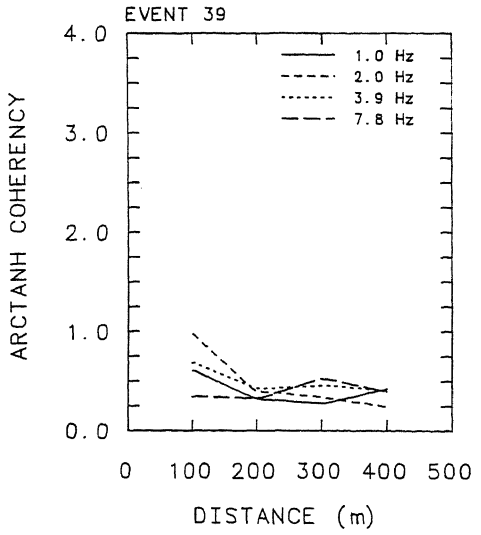

Figure 4b. The smoothed noise coherency plotted as a function of station separation.

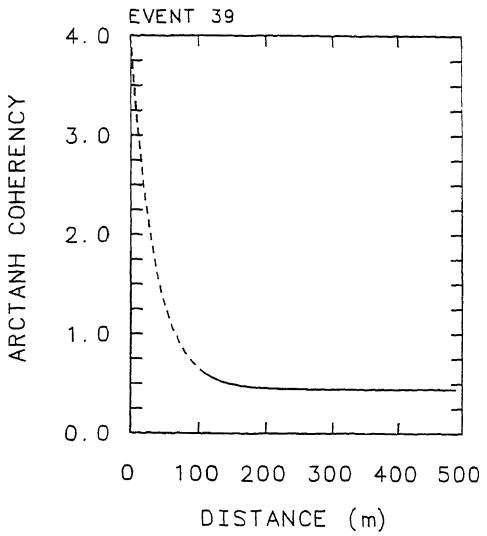

Figure 5. The empirical noise coherency function. The dashed line is the extrapolation to short station spacings.

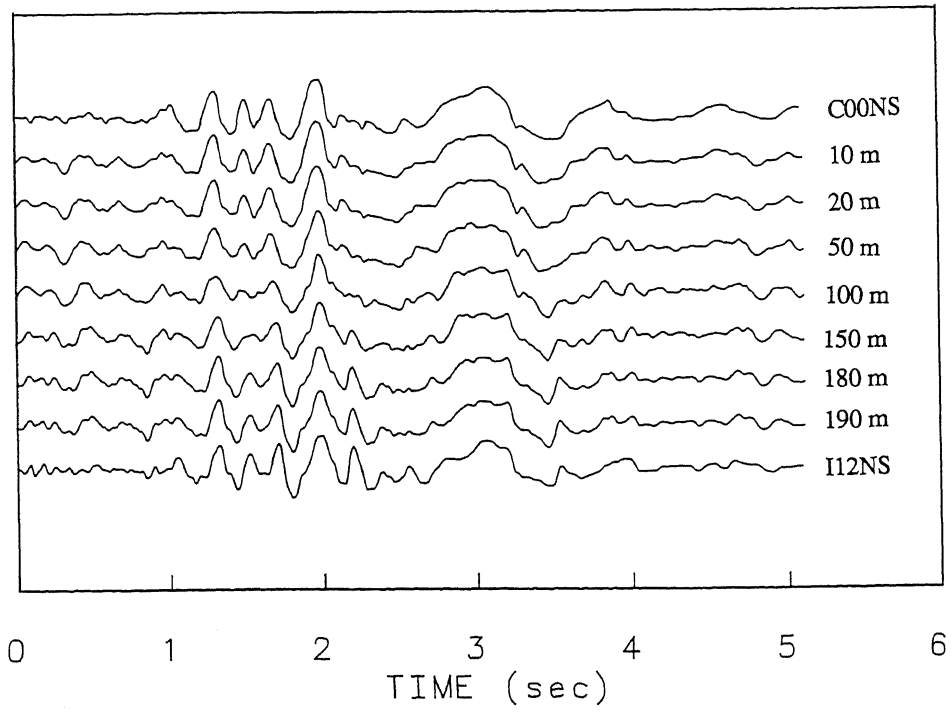

Figure 6. Interpolated accelerograms for points between station C-00 and I-12.